Gamma shielding and compressive strength analyses of polyester composites reinforced with zinc: an experiment, theoretical, and simulation based study

M. R. Kaçal[1] · H. Polat[2] · M. Oltulu[3] · F. Akman[4,5] · O. Agar[6] · H. O. Tekin[7]

Abstract

The preparation of materials with high attenuation performance is one of the major issues in the radiation shielding applications. This study is based on the investigation of gamma-shielding performances of various polyester composites reinforced with Zn. Utilizing gamma spectrometer based on HPGe detector, the mass attenuation coefficient (μ/ρ) of the present composites was measured at various photon energies between 59.5–1408 keV. The obtained experimental data were confirmed with those of MCNPX code as well as XCOM program. It is found that the attenuation coefficient values of the studied composites are in good agreement with the results of other approaches at the investigated energies. The best photon-shielding effectiveness was observed in the composite tagged with Zn (10%). The shielding characteristics of composite enhances with the addition of Zn as filler.

1 Introduction

Both X- and gamma ray photons are of ionizing electromagnetic radiation (IEMR) types and since it is mass-less and uncharged, their energies are sufficient to ionize the atoms of any material they interact with. Moreover, penetrating capabilities of X- and gamma-ray photons in material is quite high compared to other radiations [1]. It is quite possible for us or any electronic equipment to be exposed to this kind of radiation in our daily life. The most practical way to well control radiation dose to a level that cannot be harmed is to use an effective shielding material. Although lead (Pb) is superior over other metal based materials because of its high density, high atomic number and low cost, there are some important drawbacks which limit its usages and application fields [2].

Except many other absorbers such as alloy [3, 4], ceramics [5], green product [6], granite [7, 8], rocks [9] etc., composite materials which can be produced by reinforced various matrix and inorganic fillers exhibit great potential as novel shielding materials. Especially, the most preferred matrix materials as traditional shielding composites because of their efficient shielding ability, easy prepared, light weight, and multifunctional design are polymers [10]. In view of this, there are various investigations on the radiation shielding features of different polymer doped composites [11–15]. Moreover, the exposure buildup factors (EBF) are the important quantities utilized in determining the distribution of photon flux in irradiation environment. These coefficients correspond to the ratio of the total detector response

✉ O. Agar
  osmanagar@kmu.edu.tr

1   Department of Physics, Arts and Sciences Faculty, Giresun University, 28100 Giresun, Turkey

2   Department of Architecture and Urban Planning, Vocational School of Technical Sciences, Bingöl University, 12000 Bingöl, Turkey

3   Department of Civil Engineering, Engineering Faculty, Atatürk University, 25240 Erzurum, Turkey

4   Department of Property Protection and Security, Program of Occupational Health and Safety, Vocational School of Social Sciences, Bingöl University, 12000 Bingöl, Turkey

5   Central Laboratory Application and Research Center, Bingöl University, 12000 Bingöl, Turkey

6   Department of Medical Imaging Techniques, Karamanoglu Mehmetbey University, 70200 Karaman, Turkey

7   Medical Diagnostic Imaging Department, College of Health Sciences, University of Sharjah, 27272 Sharjah, United Arab Emirates

to that of un-collided photon and are used to assess the corrected response to the un-collided photons by including the contribution of the scattered photons. Among the EBF estimations, it has been found that geometric–progression (G–P) fitting technique is the most suitable to reproduce coefficients with better precision.

In this study, transition metal (namely Zn) as filling content enhances the chemical stability of material. This paper contains the detailed shielding and EBF coefficients to reveal an alternative material which consisted of light weight polymer composites for attenuation of high energetic X- and gamma-rays, as well as mechanical features of the investigated Zn-doped composites.

2 Materials and methods

2.1 Sample preparation

The unsaturated polyester (UP) and zinc (Zn) contents were used as resin and functional fillers in the synthesized polymer composites, respectively. To start and accelerate the formation process, cobalt octoate (CO) and methyl ethyl ketone peroxide (MEKP) were included as initiator and accelerator materials, respectively. At first, the essential contents were weighed in appropriate proportions with the help of the precision balance. Thereafter, the Zn filler was added to the UP resin in 2, 4, 6, 8, and 10% (Fig. 1a) by weight which was chosen based on its weight. The mixing process kept for 5 min to wet completely all the fillers. MEKP and CO were contained to the present mixture, respectively, and mixed for 3 min. It is poured into various molds that will take shape and was left to harden. Then, the composites with 2 cm diameter and 0.5, 1.0, 2.0 and 3.0 cm thicknesses (Fig. 1b) were prepared and cured in convenient conditions for 28 days. The elemental compositions and densities of the prepared Zn-doped composites are listed in Table 1.

2.2 Theoretical calculation

A photon beam with the initial intensity (I_0) after passing across the material reduces to the attenuated intensity (I). The relation of this reduction is defined by Lambert–Beer rule [16]:
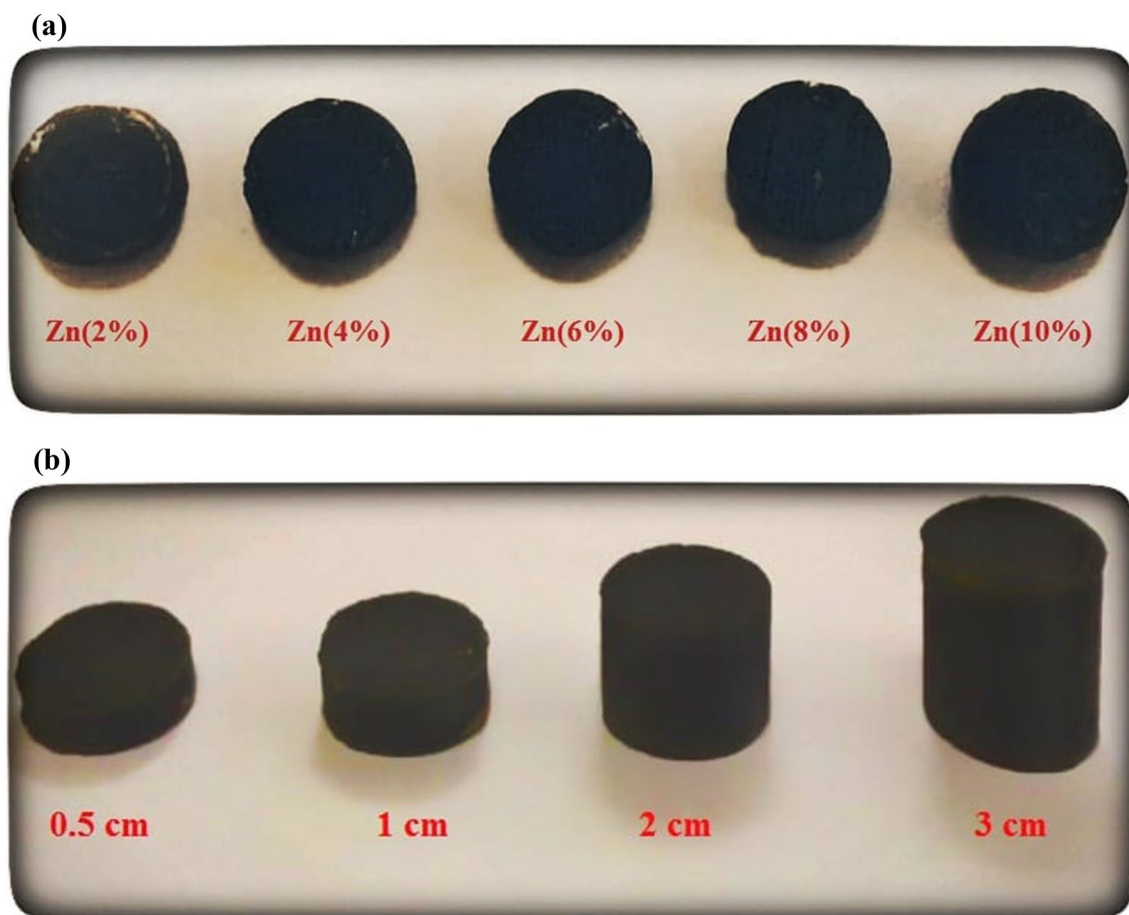
Fig. 1 Images of **a** the prepared composites and **b** Zn (10%) samples at different thicknesses

Table 1 The elemental compositions and densities of the prepared Zn-doped composites

Sample	Compositions (%)					ρ (g/cm3)
	Co	C	H	O	Zn	
Zn (2%)	0.0126	58.9899	4.4167	34.6130	1.9677	1.301
Zn (4%)	0.0126	57.8018	4.3295	33.9206	3.9353	1.305
Zn (6%)	0.0126	56.6138	4.2423	33.2283	5.9030	1.310
Zn (8%)	0.0126	55.4257	4.1550	32.5359	7.8707	1.315
Zn (10%)	0.0126	54.2377	4.0678	31.8435	9.8384	1.322

$$\mu = -\frac{\ln\frac{I}{I_0}}{x}, \tag{1}$$

where μ represents the linear attenuation coefficient (cm^{-1}) of the material and x is thickness of the sample.

After calculating μ values, mass attenuation coefficients (μ/ρ) of the studied polyester-based composites can be estimated dividing the μ with the density (ρ) of the samples [17]:

$$\mu_m = \frac{\mu}{\rho} = \sum w_i \left(\frac{\mu}{\rho}\right)_i, \tag{2}$$

where w_i and $(\mu/\rho)_i$ shows the weight fraction and mass attenuation coefficients for the individual element in any compound or mixture.

Some useful quantities e.g. total atomic and electronic cross sections, the effective atomic number and electron density, etc. can be derived with help of this parameter. The total atomic cross section (σ_a) can be determined using the following relation [18]:

$$\sigma_a = \frac{(\mu_m)}{N_A \sum_i \frac{w_i}{A_i}}. \tag{3}$$

It is expressed in cm^2/atom.

The total electronic cross section (σ_e) can be written as [19]:

$$\sigma_e = \frac{1}{N} \sum_i \mu_{mi} \frac{f_i A_i}{Z_i}, \tag{4}$$

where Z_i and f_i are the atomic number and the fractional abundance of the ith element. It is expressed in cm^2/electron.

The Z_{eff} can be derived from σ_e and σ_a [20]:

$$Z_{eff} = \frac{\sigma_a}{\sigma_e}. \tag{5}$$

The electron density (N_E) is the electron numbers per unit mass of the interacting matter and written as follows [18]:

$$N_E = (n_{tot}N)\frac{Z_{eff}}{A_{tot}}. \tag{6}$$

Half value layer (HVL) equals to the thickness of the absorber at which the intensity of the photons after travelling is minimized to 50% of the initial photon intensities. HVL (cm) can be calculated with Eq. (7) [21]:

$$HVL = \frac{\ln 2}{\mu}. \tag{7}$$

Mean free path (MFP) is a parameter that plays a significant role to calculate the exponential shielding of gamma photon. The shorter MFP for any sample means more photons interaction with this sample, hence giving shorter distance between two interactions [22]. MFP (cm) is estimated using the following relation:

$$MFP = \frac{1}{\mu}. \tag{8}$$

The radiation protection efficiency (RPE) of any material can be found by Eq. (9) [23, 24]:

$$RPE(\%) = \left(1 - \frac{I}{I_0}\right) \times 100. \tag{9}$$

The following equation is considered to estimate the experimental uncertainties in the mass attenuation coefficient analyses [25, 26]:

$$\Delta\mu_m = \frac{1}{\rho x}\sqrt{\left(\frac{\Delta I}{I}\right)^2 + \left(\frac{\Delta I_0}{I_0}\right)^2 + \ln\left(\frac{\Delta I}{I}\right)^2\left(\frac{\Delta\rho x}{\rho x}\right)^2}, \tag{10}$$

where ρ are the density of the sample, ΔI_0 and ΔI are the uncertainties for original (I_0) and attenuated (I) counts, respectively.

2.3 Shielding measurements

Photon shielding properties of the prepared polymer-based composites with various Zn amounts (2, 4, 6, 8 and 10%) are assessed experimentally by means of mass attenuation coefficients (μ/ρ) employing a high purity germanium (HPGe) detector in conjunction with multi-channel analyzer (MCA). The experimental setup and geometry of the testing equipment is represented in Fig. 2. The photo-peak energies and
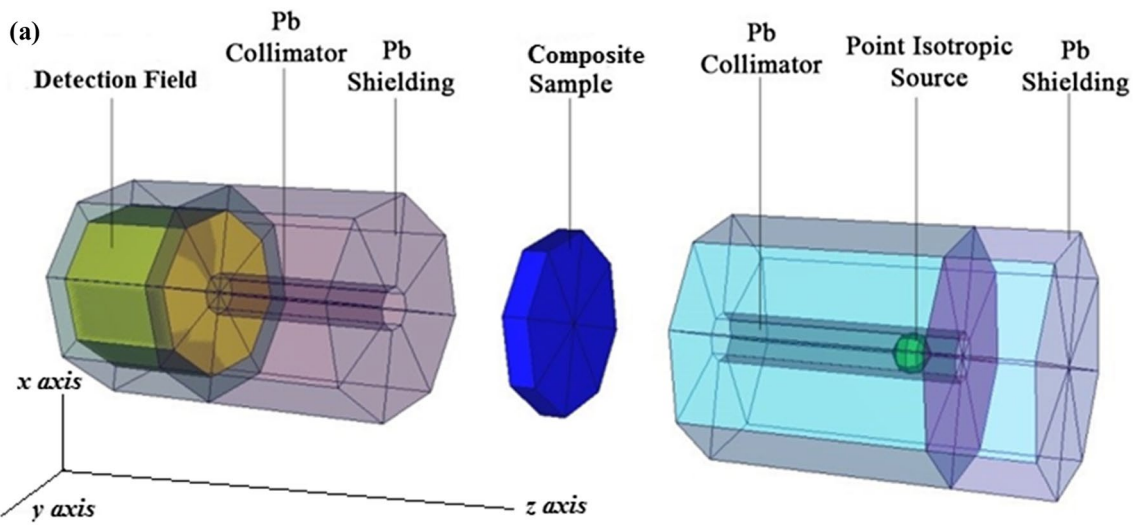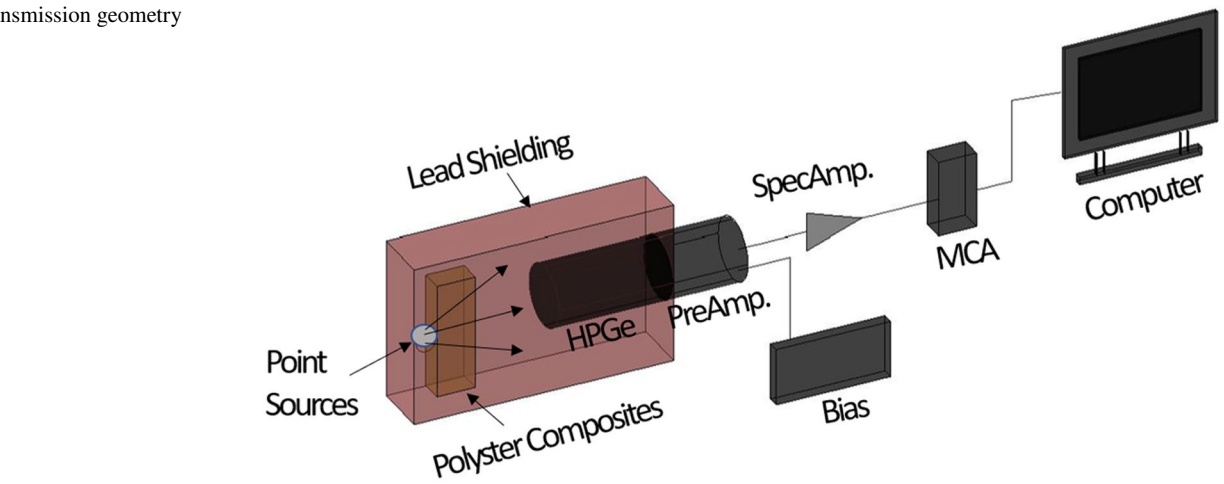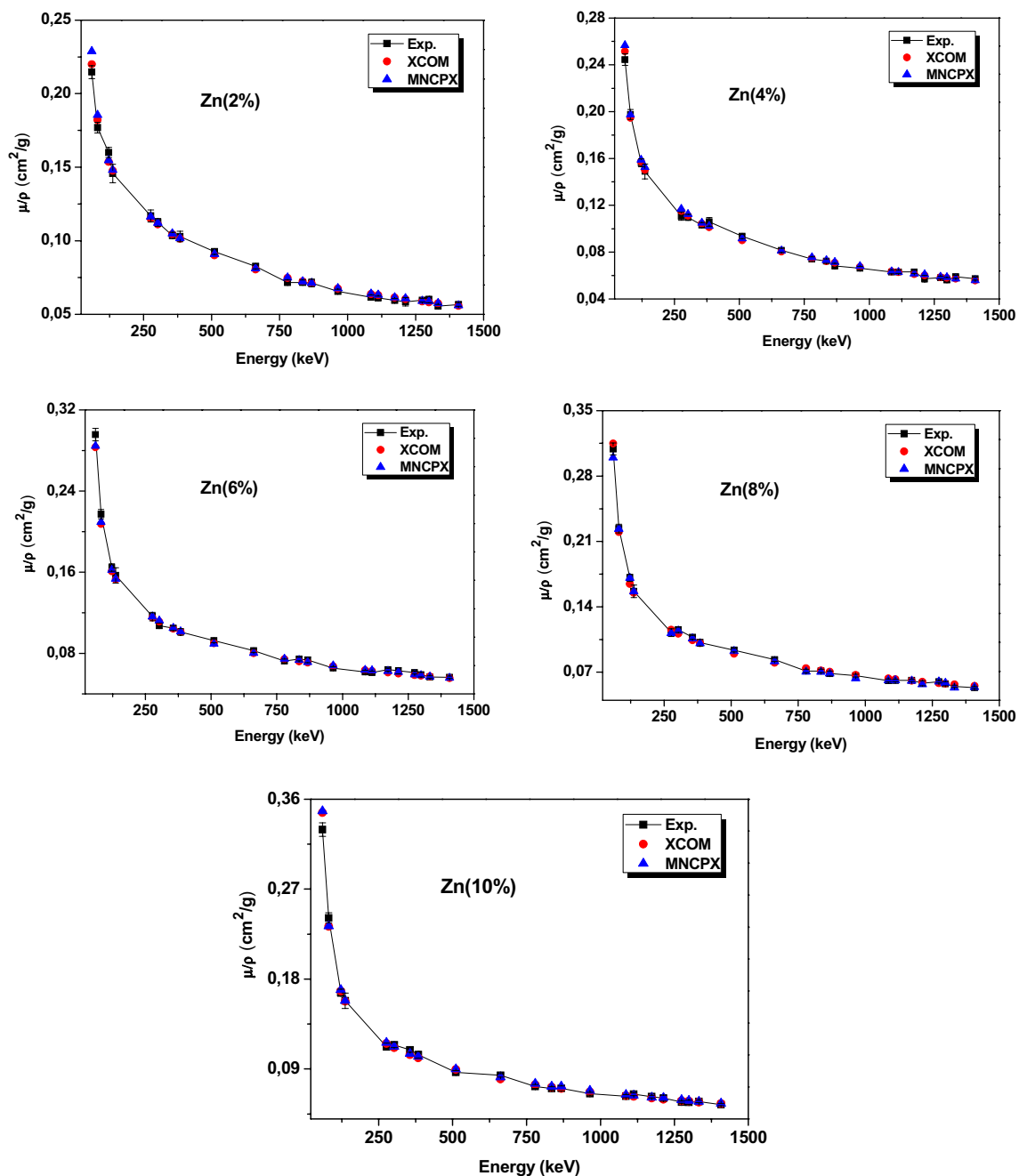
Fig. 2 Transmission geometry

Fig. 3 **a** Simulation setup of mass attenuation coefficients. **b** 3-D layout of modeled 3×3 inch NaI(Tl) detector obtained from MCNPX Visual Editor (VE X_22S)

Fig. 4 Comparison of the experimental, theoretical, and simulation mass attenuation coefficients for the studied samples

nuclear data emitted by the ^{241}Am, ^{152}Eu, ^{137}Cs, ^{133}Ba, ^{60}Co, ^{57}Co, ^{54}Mn and ^{22}Na radioactive point sources can be found from [27]. More detail information on experimental system can be taken from our previous studies [3, 4, 6]. The analysis of the observed photo-peaks in data acquisitions were done with an MAESTRO software [28, 29]. Their net areas were determined with help of the least-squares fitting method through the Origin 7.5 program (demo). On the other hand, to obtain the small differences among experimental,

theoretical, and simulation results, uncertainties in thickness of the sample, original intensity (I_0), and attenuated photon intensity (I) for attenuation coefficient values have considered as given in Eq. 10.

2.4 MCNPX calculations

Monte Carlo N-Particle Transport Code System-extended (MCNPX) has been carried out to approve the experimental

Table 2 Experimental, XCOM and MCNPX mass attenuation coefficients of Zn-based polyester composites

| Energy (keV)	Mass attenuation coefficients (cm²/g)														
	Zn (2%)			Zn (4%)			Zn (6%)			Zn (8%)			Zn (10%)		
	Exp	XCOM	MCNPX	Exp	XCOM	MCNPX	Exp	XCOM	MCNPX	Exp	XCOM	MCNPX	Exp	XCOM	MCNPX
59.5	0.215(4)	0.2200	0.2289	0.244(5)	0.2515	0.2568	0.296(6)	0.2832	0.2845	0.309(6)	0.3149	0.2996	0.330(7)	0.3466	0.3481
80.9	0.177(4)	0.1822	0.1855	0.198(4)	0.1947	0.1974	0.217(5)	0.2074	0.2095	0.224(5)	0.2200	0.2234	0.241(5)	0.2327	0.2331
122.1	0.160(3)	0.1537	0.1547	0.156(3)	0.1572	0.1588	0.165(4)	0.1608	0.1621	0.171(4)	0.1644	0.1709	0.166(4)	0.1680	0.1692
136.4	0.146(6)	0.1477	0.1481	0.149(6)	0.1502	0.1526	0.157(8)	0.1527	0.1534	0.157(7)	0.1552	0.1563	0.158(8)	0.1577	0.1585
276.3	0.117(4)	0.1150	0.1164	0.111(4)	0.1151	0.1170	0.116(4)	0.1153	0.1162	0.112(4)	0.1154	0.1118	0.112(4)	0.1155	0.1163
302.8	0.112(3)	0.1111	0.1121	0.110(3)	0.1112	0.1124	0.107(3)	0.1112	0.1123	0.115(3)	0.1113	0.1143	0.114(3)	0.1113	0.1124
356.0	0.104(2)	0.1044	0.1049	0.103(2)	0.1044	0.1051	0.105(2)	0.1043	0.1050	0.107(2)	0.1043	0.1060	0.109(2)	0.1042	0.1053
383.8	0.103(4)	0.1013	0.1017	0.106(4)	0.1013	0.1023	0.101(3)	0.1012	0.1015	0.102(4)	0.1011	0.1008	0.104(3)	0.1010	0.1026
511.0	0.093(2)	0.0901	0.0910	0.093(2)	0.0900	0.0915	0.093(2)	0.0898	0.0895	0.094(2)	0.0897	0.0926	0.087(2)	0.0896	0.0899
661.6	0.083(2)	0.0805	0.0812	0.081(2)	0.0803	0.0812	0.083(3)	0.0802	0.0804	0.083(2)	0.0801	0.0815	0.084(2)	0.0799	0.0817
778.9	0.072(2)	0.0747	0.0749	0.074(2)	0.0746	0.0756	0.072(2)	0.0744	0.0746	0.071(2)	0.0743	0.0706	0.072(2)	0.0741	0.0753
834.8	0.072(2)	0.0723	0.0723	0.072(2)	0.0722	0.0730	0.074(2)	0.0720	0.0734	0.071(2)	0.0719	0.0704	0.070(2)	0.0718	0.0725
867.3	0.071(3)	0.0710	0.0712	0.068(2)	0.0709	0.0714	0.074(3)	0.0707	0.0712	0.069(3)	0.0706	0.0685	0.071(3)	0.0705	0.0726
964.1	0.066(1)	0.0675	0.0677	0.066(1)	0.0674	0.0681	0.065(1)	0.0672	0.0680	0.066(1)	0.0671	0.0635	0.065(1)	0.0670	0.0684
1085.8	0.062(2)	0.0637	0.0639	0.063(2)	0.0636	0.0634	0.062(2)	0.0634	0.0637	0.061(2)	0.0633	0.0614	0.063(2)	0.0632	0.0642
1112.1	0.061(1)	0.0630	0.0632	0.063(1)	0.0628	0.0630	0.061(1)	0.0627	0.0632	0.061(1)	0.0626	0.0613	0.065(1)	0.0624	0.0634
1173.2	0.059(1)	0.0613	0.0615	0.063(1)	0.0612	0.0615	0.064(1)	0.0610	0.0624	0.061(1)	0.0609	0.0607	0.062(1)	0.0608	0.0616
1212.9	0.058(3)	0.0602	0.0609	0.057(3)	0.0601	0.0610	0.063(3)	0.0600	0.0615	0.058(3)	0.0599	0.0570	0.061(3)	0.0597	0.0612
1274.5	0.060(1)	0.0587	0.0591	0.058(1)	0.0586	0.0589	0.061(1)	0.0585	0.0591	0.060(1)	0.0583	0.0599	0.057(1)	0.0582	0.0590
1299.1	0.060(2)	0.0582	0.0587	0.056(2)	0.0580	0.0585	0.059(2)	0.0579	0.0583	0.058(2)	0.0578	0.0585	0.057(2)	0.0577	0.0584
1332.5	0.056(1)	0.0574	0.0575	0.059(1)	0.0573	0.0573	0.057(1)	0.0571	0.0570	0.055(1)	0.0570	0.0534	0.057(1)	0.0569	0.0573
1408.0	0.057(1)	0.0558	0.0560	0.057(1)	0.0557	0.0559	0.056(1)	0.0556	0.0558	0.054(1)	0.0554	0.0541	0.054(1)	0.0553	0.0554
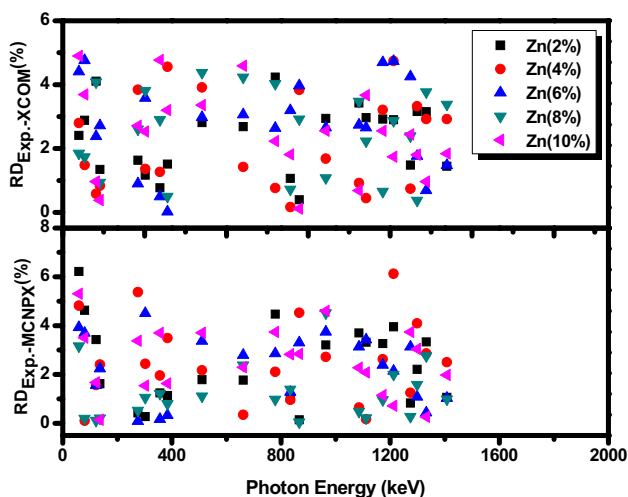
Fig. 5 The relative deviations (RD) between **a** experimental-XCOM and **b** experimental-MCNPX results
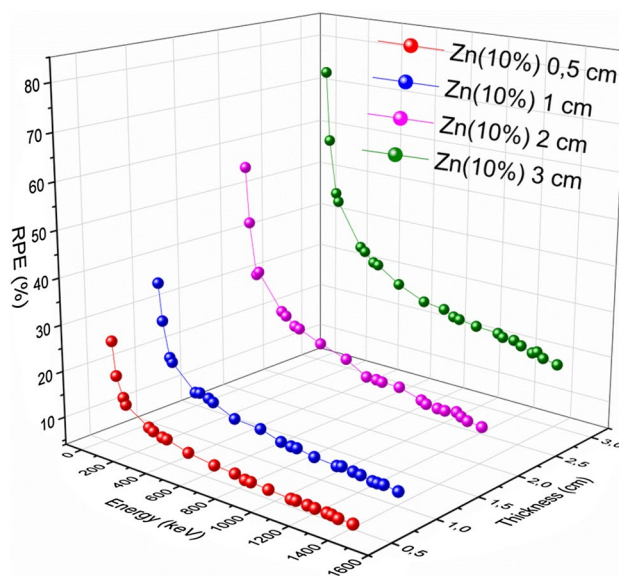

Fig. 7 Radiation protection efficiency (RPE) for the prepared composites at different thicknesses
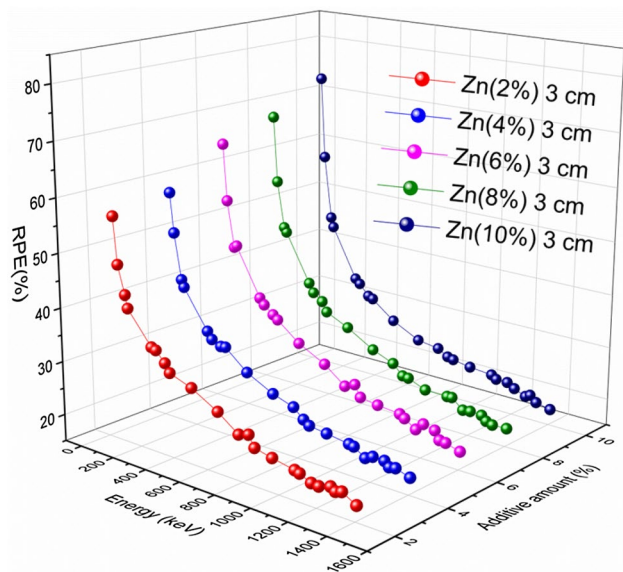

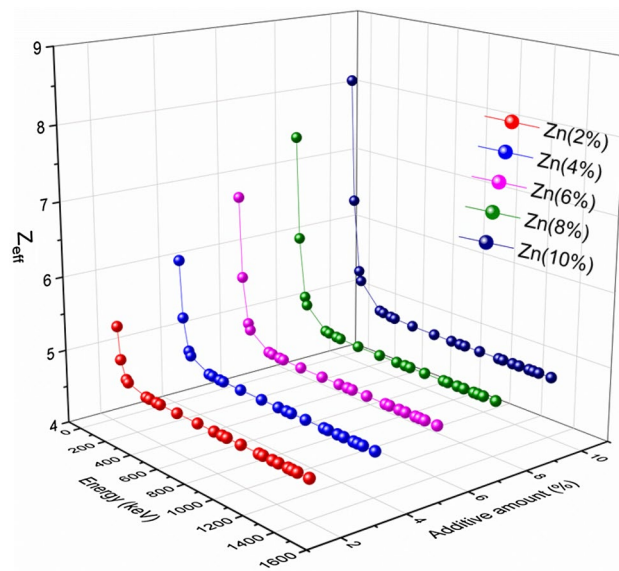**Fig. 6** Radiation protection efficiency (RPE) for the prepared composites at 3 cm thickness

Fig. 8 Comparison of effective atomic number (Z_{eff}) for the prepared composites

μ/ρ values between 59.5 and 1408 keV photon energy range. Monte Carlo N-Particle Transport Code System-extended (MCNPX) has been carried out to approve the experimental μ/ρ results. Figure 3 demonstrates the MCNPX 3-D view of photon shielding design with several simulation elements, i.e., a point radioactive source, the composite sample, Pb blocks to prevent from the scattered photons, Pb collimator for primary radiation beam and F4 tally mesh detection field. More details on simulation layout can be found from our previous studies [4, 30].

2.5 Exposure buildup factors (EBF)

The exposure buildup factors (EBF) are calculated using G–P fitting technique for incident photon energy of 0.015–10 MeV. The estimations on the EBF of the investigated composites are carried out in three steps; these are: the estimations of (a) equivalent atomic number (Z_{eq}), (b) the G–P fitting parameters (b, c, d, a and X_k) and (c) the
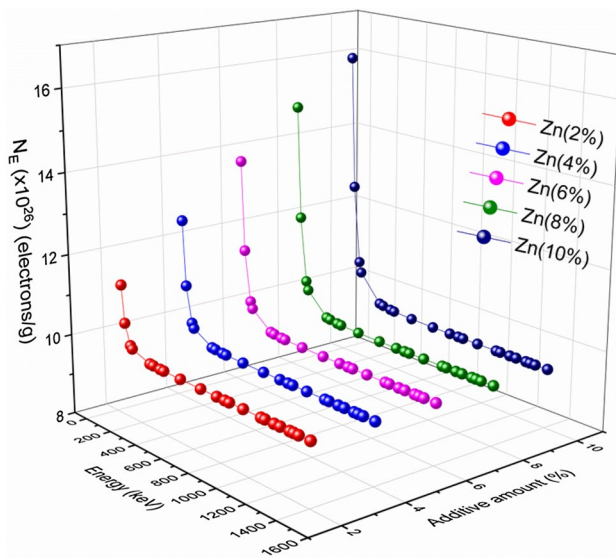
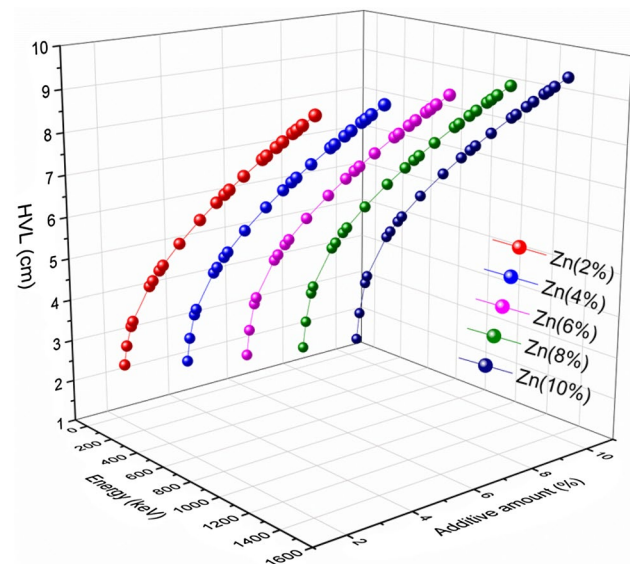**Fig. 9** Effective electron density (N_E) for the prepared composites

Fig. 11 Theoretical HVL values of different Zn-based composites
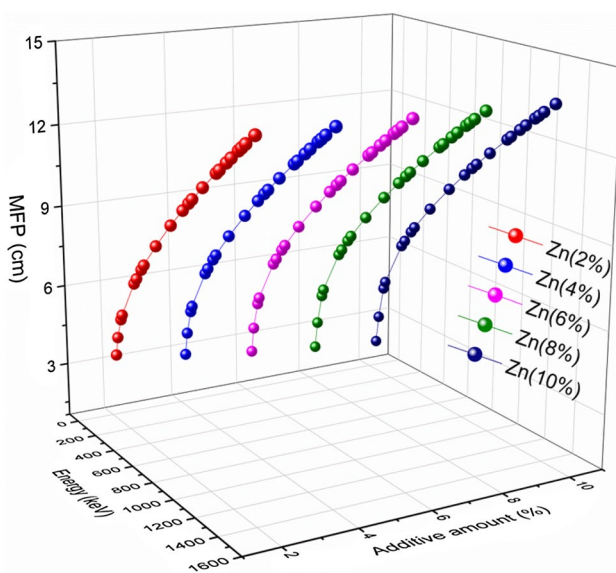

Fig. 10 Theoretical MFP values of different Zn-based composites

determination of EBF values. More details on EBF calculations can be found in our previous studies [31].

2.6 Compressive strength tests

The strength values were determined by compressive strength test on polymer composite samples. The compressive strength test was performed according to TS EN 12390-3 [32]. The compressive strengths of the cube samples were made in the press with an automatic loading speed control with a capacity of 30 tons.

3 Results and discussions

3.1 Nuclear radiation shielding performance

Mass attenuation coefficients (μ/ρ) of Zn-filled polyester based composites using the experimental and theoretical (XCOM) methods are represented in Fig. 4 and listed in Table 2. It is clear that the μ/ρ values of the studied composites dramatically reduce with the increment of photon energy, which is due to several interaction processes of gamma photons with materials. Looking at Fig. 4, the variation between μ/ρ parameter and photon energy can be evaluated in two different regions while the second region (ii) lies from 400 to 1400 keV. Along first region between 50 and 400 keV, the predominant interaction mode which is related to energy ($E^{-3.5}$) and atomic number (Z^{4-5}) is defined as photoelectric effect (PE). The energy level differences of the atoms forming composite matches the low energy photons. Therefore, this mode happens easily and leads to decrease aggressively μ/ρ values at 50 keV. In the second region ($E > 400$ keV), the possibility of PE is gradually reduced since the energy emitted by radioactive source is higher than the energy demanded for the electron transition and Compton scattering (CS) mode whose cross section is proportional to E^{-1} and Z becomes dominant. Thus, the μ/ρ values of all the composites slightly decrease with the increase of photon energy and are quite close to each other as seen in Fig. 4.

Additionally, XCOM software and MCNPX code are carried out to confirm the experimental results. The theoretical and simulation μ/ρ were estimated considering the elemental compositions of the composites at the various energies of 59.5–1408 keV. The relative deviation (RD) between mass

Table 3 Z_{eq} and G–P exposure buildup factor (EBF) coefficients for Zn (2%) based composites

Energy (MeV)	Z_{eq}	EBF				
		a	b	c	d	X_k
0.015	8.90	0.200	1.119	0.414	−0.103	13.549
0.02	9.13	0.183	1.259	0.461	−0.096	14.191
0.03	9.43	0.132	1.711	0.595	−0.070	15.458
0.04	9.62	0.062	2.350	0.800	−0.033	15.165
0.05	9.77	0.034	3.015	0.950	−0.028	14.024
0.06	9.89	−0.008	3.428	1.128	−0.009	13.430
0.08	10.05	−0.061	3.001	1.382	0.016	13.615
0.1	10.15	−0.088	3.667	1.538	0.027	14.224
0.15	10.22	−0.111	3.348	1.689	0.035	15.347
0.2	10.44	−0.114	3.026	1.703	0.035	14.531
0.3	9.84	−0.123	2.732	1.744	0.039	14.148
0.4	10.75	−0.104	2.492	1.604	0.030	15.026
0.5	10.74	−0.100	2.360	1.561	0.032	14.810
0.6	10.37	−0.095	2.273	1.523	0.030	15.216
0.8	9.90	−0.088	2.140	1.458	0.031	14.869
1	8.91	−0.079	2.073	1.397	0.030	14.807
1.5	7.30	−0.058	1.956	1.268	0.024	14.698
2	6.74	−0.041	1.868	1.180	0.018	13.960
3	6.67	−0.014	1.729	1.060	0.005	13.331
4	6.68	0.004	1.638	0.988	−0.006	18.720
5	6.68	0.018	1.621	0.940	−0.012	13.860
6	6.68	0.029	1.519	0.903	−0.017	13.042
8	6.67	0.035	1.428	0.881	−0.022	13.364
10	6.66	0.039	1.365	0.867	−0.022	13.601
15	6.65	0.046	1.273	0.841	−0.032	15.116

attenuation coefficients through experimental and XCOM as well as MCNPX can be calculated as below relation [19, 33]:

$$RD(\%) = \left| \left(\frac{\frac{\mu}{\rho}_{exp} - \frac{\mu}{\rho}_{XCOM,MCNPX}}{\frac{\mu}{\rho}_{exp}} \right) \right| \times 100. \qquad (11)$$

As plotted in Fig. 5, RD values of different composites at certain photon energies are found to be 0.02–4.92% and 0.05–6.22% for experimental-XCOM and experimental-MCNPX, respectively, and it is clear seen that they are quite compatible. The two main reasons of very minor discrepancy between two methods: (i) detecting a part of the scattered photons with low scattering angle by the detector due to the narrow beam system (ii) to the mixture rule that disregards the interactions among atoms forming material.

The RPE parameter corresponds to the measure on photons that can be attenuated by the polymer based composite and can be calculated with help of the intensities of initial

and attenuated photons for the polymer composites at the studied energies. The obtained results are graphically demonstrated in Fig. 6. It is clear from this figure that the polymer composites possess high shielding performance at low energy. Among the synthesized composites, the highest RPE value is observed to be 72.04% for the Zn (10%) sample at 59.5 keV and 3 cm thickness. Additionally, gamma spectra measurements were obtained for Zn (10%) with different thicknesses of 0.5, 1, 2 and 3 cm and their RPEs were determined (Fig. 7). This parameter is proportional to the thickness of the material. Moreover, it can be easily said from Figs. 6 and 7 that it minimizes with the increase in energy. Therefore, we can deduce that the Zn (10%) has best attenuating performance than the rest of the other polymer composites, and all absorbers are more effective for shielding the low energy photons.

The Z_{eff} attitudes of the Zn-based composites towards photon energies are plotted in Fig. 8. These results are varying with photon energies form 59.5 to 1408 keV. From Fig. 8, there is increasing order of Z_{eff}: Zn (2%) > Zn (4%) > Zn (6%) > Zn (8%) > Zn (10%). The composite tagged as Zn (10%) has the highest Z_{eff} at all the analyzed energies and may be resulting from possessing a maximum

Table 4 Z_{eq} and G–P exposure buildup factor (EBF) coefficients for Zn (4%) based composites

Energy (MeV)	Z_{eq}	EBF				
		a	b	c	d	X_k
0.015	10.24	0.215	1.075	0.391	−0.111	12.322
0.02	10.54	0.205	1.153	0.412	−0.110	13.688
0.03	10.93	0.174	1.400	0.484	−0.091	14.633
0.04	11.20	0.108	1.746	0.641	−0.054	16.159
0.05	11.38	0.102	2.279	0.698	−0.059	14.248
0.06	11.52	0.055	2.642	0.849	−0.046	14.134
0.08	11.72	−0.004	2.774	1.078	−0.015	13.665
0.1	11.88	−0.038	3.136	1.246	−0.002	12.536
0.15	12.12	−0.073	3.013	1.442	0.013	15.905
0.2	12.20	−0.085	2.837	1.520	0.018	16.200
0.3	13.20	−0.084	2.533	1.501	0.016	16.360
0.4	12.43	−0.090	2.422	1.522	0.022	15.887
0.5	12.32	−0.087	2.306	1.495	0.022	16.135
0.6	12.73	−0.082	2.203	1.455	0.023	16.567
0.8	12.73	−0.073	2.085	1.388	0.021	16.082
1	11.90	−0.069	2.006	1.351	0.023	15.691
1.5	7.79	−0.057	1.937	1.266	0.024	14.521
2	7.10	−0.040	1.856	1.175	0.017	14.097
3	7.18	−0.013	1.717	1.059	0.004	13.748
4	7.12	0.004	1.630	0.989	−0.005	16.247
5	7.07	0.018	1.561	0.941	−0.013	13.644
6	7.08	0.030	1.516	0.902	−0.019	12.716
8	7.06	0.033	1.423	0.887	−0.016	11.710
10	7.06	0.037	1.361	0.873	−0.022	14.195
15	7.04	0.048	1.271	0.841	−0.034	15.040

Table 5 Z_{eq} and G–P exposure buildup factor (EBF) coefficients for Zn (6%) based composites

Energy (MeV)	Z_{eq}	EBF				
		a	b	c	d	X_k
0.015	11.26	0.220	1.048	0.385	−0.120	12.124
0.02	11.61	0.191	1.099	0.424	−0.100	14.039
0.03	12.06	0.190	1.284	0.447	−0.102	14.421
0.04	12.35	0.151	1.567	0.537	−0.081	15.028
0.05	12.56	0.110	1.910	0.652	−0.056	15.389
0.06	12.72	0.095	2.266	0.724	−0.058	13.455
0.08	12.96	0.034	2.651	0.928	−0.035	13.015
0.1	13.10	−0.007	2.825	1.101	−0.020	13.048
0.15	13.34	−0.052	2.827	1.328	0.002	17.801
0.2	13.44	−0.067	2.723	1.419	0.004	12.815
0.3	13.54	−0.081	2.511	1.487	0.015	16.591
0.4	13.83	−0.082	2.363	1.477	0.017	15.922
0.5	14.04	−0.080	2.251	1.454	0.018	16.300
0.6	13.62	−0.078	2.184	1.433	0.022	18.055
0.8	13.88	−0.073	2.056	1.385	0.021	15.396
1	12.80	−0.067	1.996	1.339	0.022	15.819
1.5	8.95	−0.054	1.911	1.254	0.021	14.717
2	7.70	−0.037	1.843	1.167	0.015	14.981
3	7.58	−0.012	1.714	1.056	0.003	13.309
4	7.52	0.004	1.627	0.990	−0.006	18.255
5	7.50	0.017	1.557	0.944	−0.012	14.011
6	7.50	0.027	1.511	0.909	−0.021	14.097
8	7.49	0.033	1.420	0.889	−0.018	11.986
10	7.48	0.038	1.360	0.873	−0.024	14.101
15	7.44	0.049	1.268	0.841	−0.036	15.035

Table 6 Z_{eq} and G–P exposure buildup factor (EBF) coefficients for Zn (8%) based composites

Energy (MeV)	Z_{eq}	EBF				
		a	b	c	d	X_k
0.015	12.10	0.210	1.036	0.400	−0.134	13.561
0.02	12.50	0.199	1.076	0.411	−0.106	14.070
0.03	12.98	0.198	1.224	0.423	−0.104	15.084
0.04	13.30	0.173	1.451	0.490	−0.095	14.643
0.05	13.52	0.118	1.699	0.620	−0.061	15.694
0.06	13.69	0.096	1.984	0.700	−0.054	14.561
0.08	13.94	0.057	2.415	0.843	−0.050	14.559
0.1	14.09	0.014	2.610	1.011	−0.031	13.687
0.15	14.33	−0.037	2.691	1.247	−0.009	10.831
0.2	14.52	−0.053	2.631	1.345	−0.007	8.411
0.3	14.70	−0.074	2.446	1.443	0.013	18.506
0.4	14.81	−0.076	2.330	1.446	0.014	16.924
0.5	14.90	−0.076	2.227	1.435	0.016	16.309
0.6	15.01	−0.075	2.147	1.416	0.018	16.454
0.8	15.18	−0.070	2.034	1.371	0.020	15.816
1	14.71	−0.063	1.965	1.323	0.020	16.682
1.5	9.77	−0.052	1.898	1.246	0.019	14.927
2	8.10	−0.036	1.835	1.164	0.014	15.364
3	8.05	−0.011	1.710	1.052	0.002	12.832
4	7.93	0.004	1.624	0.990	−0.007	20.161
5	7.92	0.016	1.554	0.947	−0.011	14.360
6	7.92	0.025	1.506	0.916	−0.023	15.389
8	7.89	0.033	1.418	0.891	−0.019	12.232
10	7.87	0.039	1.358	0.872	−0.025	14.016
15	7.85	0.050	1.266	0.842	−0.038	15.031

proportion of Zn. Higher Z_{eff} values of Zn (10%) indicate that it interacts with more gamma photons. Hence, while gamma photons have the lowest penetrating value through Zn (10%), photon penetration is highest in Zn (2%) sample. Moreover, one can easily understand from this figure that the Z_{eff} reduces with the increasing of the energy for the prepared composites. These trends in Z_{eff} depending on the energy are in good agreement with the data reported by Akman et al. [6] and Sharma et al. [11]. Additionally, the behaviors of N_{eff} versus energy are almost similar to those of Z_{eff} on account of inversely proportional to the mean atomic weight of the composite as viewed in Fig. 9. Therefore, Zn (2%) and Zn (10%) composites with lower and larger atomic weights have lowest and highest N_{eff} values.

MFP parameter is significant in terms of directly and shortly revealing the attenuation performance of any material investigated to minimize radiation dose to an admissible level for environment health. Lowering MFP values of any composite material, corresponds to effective shield absorber. Figure 10 displays the results for MFP for Zn doped polyester composites. It is obvious that the changes of the MFP are found to be linearly dependent upon photon energy for the synthesized composites. It is observed that the highest

and lowest values of MFP are Zn (2%) and Zn (10%) with densities of 1.301 and 1.322 g/cm³ (Table 1), respectively. It can be easily deduced that the MFP parameter is related to densities of materials and thus, the shielding performance is proportional to its density.

The HVL values of the Zn reinforced composites are estimated utilizing Eq. (8). Figure 11 demonstrated the variation in HVL data towards photon energy between 59.5 and 1408 keV. Similar to Fig. 10, HVLs of these samples aggressively increase depending on energy. The HVLs of the Zn (2%) > Zn (4%) > Zn (6%) > Zn (8%) > Zn (10%) composites are found to be 6.62, 6.61, 6.59, 6.58 and 6.56 cm at 661.6 keV, respectively. Therefore, the increase in the density as a result of containing Zn content enhances more than about 10% HVL decrease.

3.2 Dependence of EBF values on incident photon energy

Tables 3, 4, 5, 6 and 7 tabulates the calculated equivalent atomic number (Z_{eq}) and EBF G-P fitting coefficient values for Zn (2%), Zn (4%), Zn (6%), Zn (8%) and Zn (10%)

Table 7 Z_{eq} and G–P exposure buildup factor (EBF) coefficients for Zn (10%) based composites

Energy (MeV)	Z_{eq}	EBF				
		a	b	c	d	X_k
0.015	12.85	0.207	1.030	0.395	− 0.138	15.185
0.02	13.27	0.209	1.063	0.396	− 0.117	14.870
0.03	13.78	0.212	1.188	0.401	− 0.114	14.229
0.04	14.11	0.189	1.377	0.514	− 0.107	14.341
0.05	14.34	0.145	1.602	0.558	− 0.078	14.968
0.06	14.52	0.105	1.819	0.666	− 0.058	15.021
0.08	14.77	0.078	2.249	0.775	− 0.051	13.331
0.1	14.94	0.030	2.445	0.944	− 0.040	14.046
0.15	15.22	− 0.024	2.584	1.183	− 0.015	11.889
0.2	15.44	− 0.044	2.550	1.297	− 0.010	9.902
0.3	15.47	− 0.064	2.420	1.400	0.002	13.765
0.4	15.62	− 0.073	2.300	1.426	0.015	19.216
0.5	15.72	− 0.074	2.207	1.420	0.015	16.288
0.6	15.86	− 0.071	2.137	1.395	0.016	17.841
0.8	15.88	− 0.067	2.030	1.356	0.017	16.481
1	15.77	− 0.061	1.953	1.315	0.018	16.117
1.5	10.27	− 0.051	1.890	1.241	0.018	15.046
2	8.64	− 0.036	1.827	1.162	0.013	15.167
3	8.42	− 0.011	1.707	1.053	0.002	12.489
4	8.37	0.004	1.621	0.990	− 0.007	19.397
5	8.35	0.016	1.551	0.948	− 0.012	14.526
6	8.34	0.026	1.504	0.917	− 0.023	15.082
8	8.31	0.033	1.416	0.892	− 0.020	12.446
10	8.29	0.039	1.357	0.872	− 0.026	13.901
15	8.26	0.051	1.265	0.840	− 0.040	14.961

composites against photon energies of 0.015–10 MeV, respectively. The variation of equivalent atomic number (Z_{eq}) values as a function of photon energy for composite
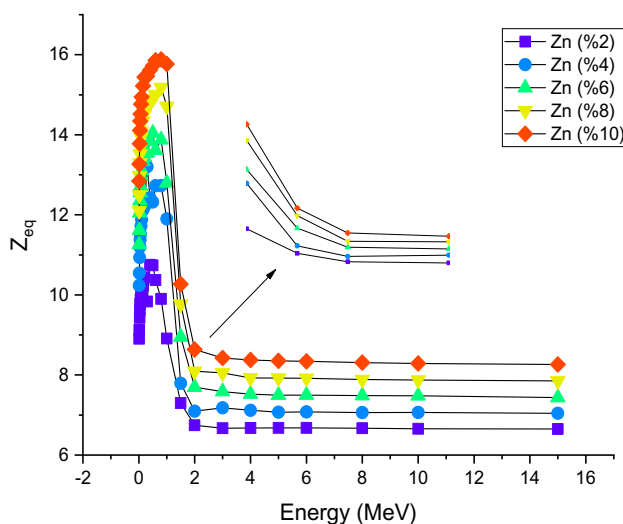

Fig. 12 Variation of equivalent atomic number (Z_{eq}) values as a function of photon energy for composite samples

samples is presented in Fig. 12. Additionally, the changes in EBF depending on incident photon energy at penetration depths such as 1, 5, 10, 20, 30 and 40 mean free paths are graphically represented in Fig. 13. It is clear that the EBF possess low values in lower photon energy region. Similar to shielding quantities, the EBF trend demonstrated in Fig. 13 can be ascribed by partial photon interaction modes. At the low energies, as PE mode dominates, photons are removed or absorbed; thus possibility of the scattering is quite small. Subsequently, since CS mechanism is predominant at the intermediate energies, the EBF leads to a larger proportion of multiple scattering over absorption. It causes a reduction of photon energy without exact annihilation of the photon, thence the higher EBF.

3.3 Compressive strength analysis

When the strength values given in Fig. 14 are examined, it is seen that when zinc powder is added at 2% of polymer weight, the increased rate increases the pressure strength by 7% compared to the control. This result can be explained that zinc powder can provide a more compact structure in the composites and increase the strength. As Zn powder ratio

Fig. 13 The changes in EBF with penetration depth at different photon energies
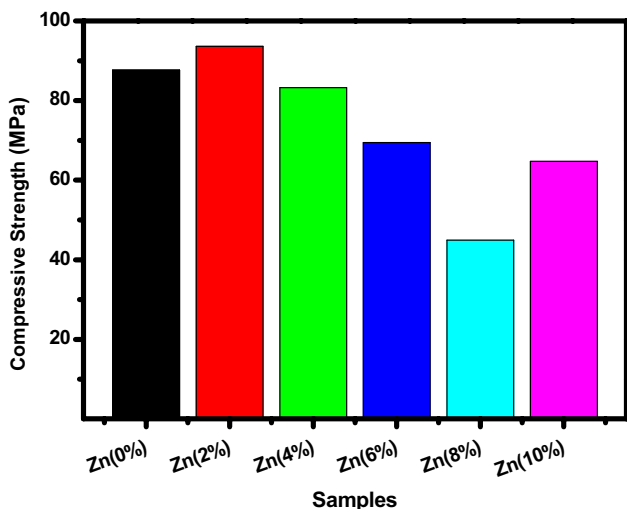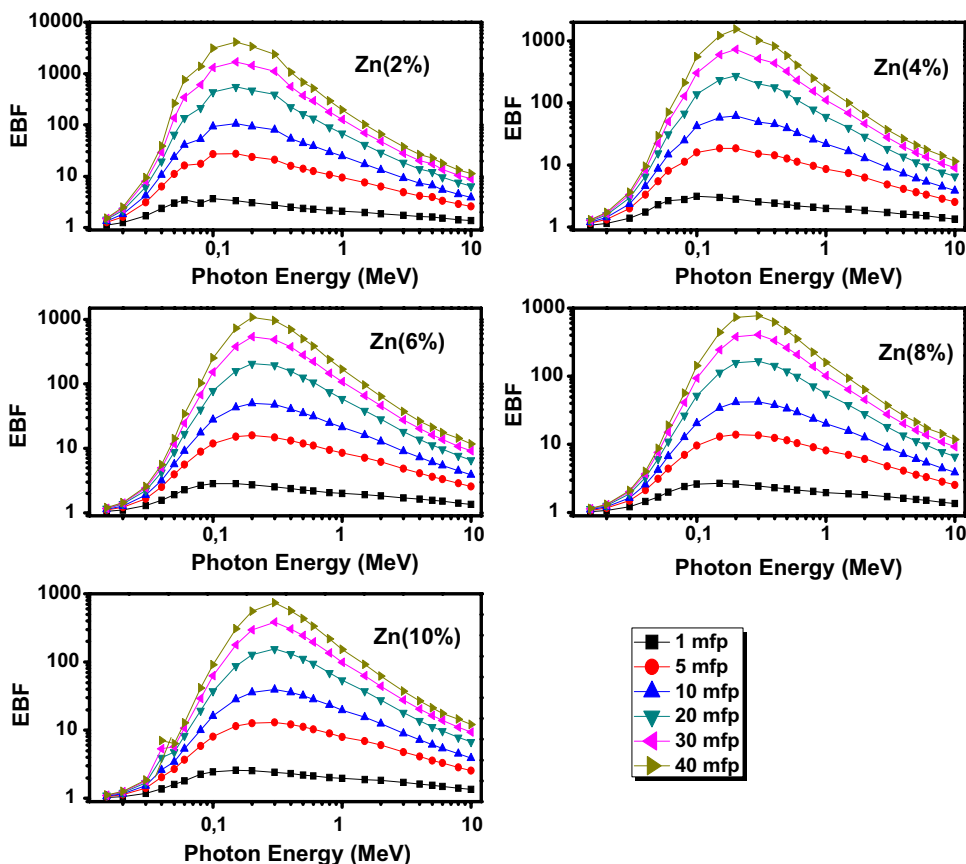
Fig. 14 Compressive strength results

increases, strength decreases. This reduction in the use of 8% Zn powder has reached up to 49%. When the data were examined, the best results were obtained from polymer composites produced using 2% Zn powder.

4 Conclusions

In this study, the attenuation and compressive strength properties of Zn-based composites with the compositions (where % = 2, 4, 6, 8 and 10) have been investigated. Experimental μ_m values determined by gamma spectrometer in the photon energy range of 59.5–1408 keV were confirmed with MCNPX code and XCOM software. From Z_{eff}, MFP and HVL results, the adding of Zn content to composite possesses a positive impact on photon shielding characteristics. Therefore, it has been found that Zn (10%) composite containing high amount of Zn has superior gamma radiation shielding effectiveness than the rest of the prepared samples. Moreover, G-P method in calculation of EBF at further deep penetrations for different absorbers can be employed in many works since the collected data will be helpful in the confirmation of ANSI/ANS 6.4.3-1991 standards. Consequently, this composite may be considered as an alternative protective material for photon attenuation practices due to its superior in light weight, easy manufacturing, high mechanical performance, and designability.

References

1. E. Eren Belgin, G.A. Aycik, A. Kalemtas, A. Pelit, D.A. Dilek, M.T. Kavak, Preparation and characterization of a novel ionizing electromagnetic radiation shielding material: hematite filled polyester based composites. Radiat. Phys. Chem. (2015). https://doi.org/10.1016/j.radphyschem.2015.06.008

2. E. Eren Belgin, G.A. Aycik, Preparation and radiation attenuation performances of metal oxide filled polyethylene based composites for ionizing electromagnetic radiation shielding applications. J. Radioanal. Nucl. Chem. (2015). https://doi.org/10.1007/s10967-015-4052-2

3. O. Agar, M.I. Sayyed, F. Akman, H.O. Tekin, M.R. Kaçal, An extensive investigation on gamma ray shielding features of Pd/Ag-based alloys. Nucl. Eng. Technol. (2018). https://doi.org/10.1016/j.net.2018.12.014

4. F. Akman, M.I. Sayyed, M.R. Kaçal, H.O. Tekin, Investigation of photon shielding performances of some selected alloys by experimental data, theoretical and MCNPX code in the energy range of 81 keV–1333 keV. J. Alloys Compd. (2019). https://doi.org/10.1016/j.jallcom.2018.09.177

5. M.I. Sayyed, F. Akman, A. Kumar, M.R. Kaçal, Evaluation of radioprotection properties of some selected ceramic samples. Results Phys. **11**, 1100–1104 (2018). https://doi.org/10.1016/j.rinp.2018.11.028

6. F. Akman, O. Agar, M.R. Kaçal, M.I. Sayyed, Comparison of experimental and theoretical radiation shielding parameters of several environmentally friendly materials. Nucl. Sci. Tech. (2019). https://doi.org/10.1007/s41365-019-0631-1

7. C. Eke, O. Agar, C. Segebade, I. Boztosun, Attenuation properties of radiation shielding materials such as granite and marble against γ-ray energies between 80 and 1350 keV. Radiochim. Acta. (2017). https://doi.org/10.1515/ract-2016-2690

8. H.O. Tekin, T.T. Erguzel, M.I. Sayyed, V.P. Singh, T. Manici, E.E. Altunsoy, O. Agar, An investigation on shielding properties of different granite samples using MCNPX code. Dig. J. Nanomater. Biostruct. **13**, 381–389 (2018)

9. S.S. Obaid, M.I. Sayyed, D.K. Gaikwad, P.P. Pawar, Attenuation coefficients and exposure buildup factor of some rocks for gamma ray shielding applications. Radiat. Phys. Chem. (2018). https://doi.org/10.1016/j.radphyschem.2018.02.026

10. R. Li, Y. Gu, Y. Wang, Z. Yang, M. Li, Z. Zhang, Effect of particle size on gamma radiation shielding property of gadolinium oxide dispersed epoxy resin matrix composite. Mater. Res. Express (2017). https://doi.org/10.1088/2053-1591/aa6651

11. A. Sharma, M.I. Sayyed, O. Agar, M.R. Kaçal, H. Polat, F. Akman, Photon-shielding performance of bismuth oxychloride-filled polyester concretes. Mater. Chem. Phys. **241**, 122330 (2020). https://doi.org/10.1016/j.matchemphys.2019.122330

12. R. Li, Y. Gu, G. Zhang, Z. Yang, M. Li, Z. Zhang, Radiation shielding property of structural polymer composite: Continuous basalt fiber reinforced epoxy matrix composite containing erbium oxide. Compos. Sci. Technol. (2017). https://doi.org/10.1016/j.compscitech.2017.03.002

13. S. Nambiar, J.T.W. Yeow, Polymer-composite materials for radiation protection. ACS Appl. Mater. Interfaces (2012). https://doi.org/10.1021/am300783d

14. M.R. Ambika, N. Nagaiah, S.K. Suman, Role of bismuth oxide as a reinforcer on gamma shielding ability of unsaturated polyester based polymer composites. J. Appl. Polym. Sci. (2017). https://doi.org/10.1002/app.44657

15. R. Mirji, B. Lobo, Computation of the mass attenuation coefficient of polymeric materials at specific gamma photon energies. Radiat. Phys. Chem. (2017). https://doi.org/10.1016/j.radphyschem.2017.03.001

16. M.I. Sayyed, F. Akman, I.H. Geçibesler, H.O. Tekin, Measurement of mass attenuation coefficients, effective atomic numbers, and electron densities for different parts of medicinal aromatic plants in low-energy region. Nucl. Sci. Tech. (2018). https://doi.org/10.1007/s41365-018-0475-0

17. F. Akman, M.R. Kaçal, M.I. Sayyed, H.A. Karataş, Study of gamma radiation attenuation properties of some selected ternary alloys. J. Alloys Compd. **782**, 315–322 (2019). https://doi.org/10.1016/j.jallcom.2018.12.221

18. F. Akman, R. Durak, M.F. Turhan, M.R. Kaçal, Studies on effective atomic numbers, electron densities from mass attenuation coefficients near the K edge in some samarium compounds. Appl. Radiat. Isot. (2015). https://doi.org/10.1016/j.apradiso.2015.04.001

19. M.G. Dong, O. Agar, H.O. Tekin, O. Kilicoglu, K.M. Kaky, M.I. Sayyed, A comparative study on gamma photon shielding features of various germanate glass systems. Compos. Part B Eng. **165**, 636–647 (2019). https://doi.org/10.1016/j.compositesb.2019.02.022

20. F. Akman, M.R. Kaçal, N. Almousa, M.I. Sayyed, H. Polat, Gamma-ray attenuation parameters for polymer composites reinforced with $BaTiO_3$ and $CaWO_4$ compounds. Prog. Nucl. Energy. (2020). https://doi.org/10.1016/j.pnucene.2020.103257

21. N.S. Prabhu, V. Hegde, A. Wagh, M.I. Sayyed, O. Agar, S.D. Kamath, Physical, structural and optical properties of Sm 3+ doped lithium zinc alumino borate glasses. J. Non Cryst. Solids **515**, 116–124 (2019). https://doi.org/10.1016/j.jnoncrysol.2019.04.015

22. N.S. Prabhu, V. Hegde, M.I. Sayyed, O. Agar, S.D. Kamath, Investigations on structural and radiation shielding properties of Er^{3+} doped zinc bismuth borate glasses. Mater. Chem. Phys. **230**, 267–276 (2019). https://doi.org/10.1016/j.matchemphys.2019.03.074

23. M.I. Sayyed, H.O. Tekin, O. Kılıcoglu, O. Agar, M.H.M. Zaid, Shielding features of concrete types containing sepiolite mineral: comprehensive study on experimental. XCOM and MCNPX results. Results Phys. (2018). https://doi.org/10.1016/j.rinp.2018.08.029

24. A. Kumar, Gamma ray shielding properties of PbO-Li_2O-B_2O_3 glasses. Radiat. Phys. Chem. **136**, 50–53 (2017). https://doi.org/10.1016/j.radphyschem.2017.03.023

25. F. Akman, I.H. Geçibesler, M.I. Sayyed, S.A. Tijani, A.R. Tufekci, I. Demirtas, Determination of some useful radiation interaction parameters for waste foods. Nucl. Eng. Technol. (2018). https://doi.org/10.1016/j.net.2018.05.007

26. H.S. Mann, G.S. Brar, K.S. Mann, G.S. Mudahar, Experimental Investigation of clay fly ash bricks for gamma-ray shielding. Nucl. Eng. Technol. **48**, 1230–1236 (2016). https://doi.org/10.1016/j.net.2016.04.001

27. National Nuclear Data Center (NNDC) in Brookhaven National Laboratory, National Nuclear Data Center (NNDC) in Brookhaven National Laboratory (n.d.). https://www.nndc.bnl.gov/nudat2/

28. Maestro, No Title (2018). www.Ortec-Online.Com/Download/Maest

29. O. Agar, I. Boztosun, C. Segebade, Multielemental analysis of some soils in Karaman by PAA using a cLINAC. Appl. Radiat. Isot. **122**, 57–62 (2017). https://doi.org/10.1016/j.apradiso.2017.01.011

30. O. Agar, Z.Y. Khattari, M.I. Sayyed, H.O. Tekin, S. Al-Omari, M. Maghrabi, M.H.M. Zaid, I.V. Kityk, Evaluation of the shielding parameters of alkaline earth based phosphate glasses using MCNPX code. Results Phys. **12**, 101–106 (2019). https://doi.org/10.1016/j.rinp.2018.11.054

31. M.I. Sayyed, H.O. Tekin, O. Agar, Gamma photon and neutron attenuation properties of MgO–BaO–B_2O_3–TeO_2–Cr_2O_3

glasses: The role of TeO_2. Radiat. Phys. Chem. (2019). https://doi.org/10.1016/j.radphyschem.2019.05.012

32. TS EN 12390-3, Concrete-hardened concrete tests—part 3: determination of compressive strength of test samples, Ankara (2010)
33. O. Agar, M.I. Sayyed, H.O. Tekin, K.M. Kaky, S.O. Baki, I. Kityk, An investigation on shielding properties of BaO, MoO_3 and P_2O_5 based glasses using MCNPX code. Results Phys. **12**, 629–634 (2019). https://doi.org/10.1016/j.rinp.2018.12.003